![ChemComm journal cover. Volume 1 | Number 1 | Jan 2013 | Pages 1–100. ChemComm, Chemical Communications, www.rsc.org/chemcomm. Royal Society of Chemistry.](image)

Volume 1 | Number 1 | Jan 2013 | Pages 1–100

ChemComm

Chemical Communications
www.rsc.org/chemcomm

ROYAL SOCIETY OF CHEMISTRY

This is an *Accepted Manuscript*, which has been through the Royal Society of Chemistry peer review process and has been accepted for publication.

Accepted Manuscripts are published online shortly after acceptance, before technical editing, formatting and proof reading. Using this free service, authors can make their results available to the community, in citable form, before we publish the edited article. We will replace this *Accepted Manuscript* with the edited and formatted *Advance Article* as soon as it is available.

You can find more information about *Accepted Manuscripts* in the **Information for Authors**.

Please note that technical editing may introduce minor changes to the text and/or graphics, which may alter content. The journal's standard **Terms & Conditions** and the **Ethical guidelines** still apply. In no event shall the Royal Society of Chemistry be held responsible for any errors or omissions in this *Accepted Manuscript* or any consequences arising from the use of any information it contains.

Journal Name

ChemComm

ARTICLE TYPE

Surface Confined Synthesis of Porphyrin Containing Two-Dimensional Polymers: the Effect of Rigidity and Preferential Adsorption of Building Blocks

Xiuling Sun[a], Lixia Fan[a], Xin Zhou[b*], Wei Quan Tian[b], Zongxia Guo[c*], Zhibo Li[c], Xiaokang Li[d], Shengbin
5 **Lei[a*]**

Abstract We have designed and synthesized two porphyrin containing two-dimensional (2D) polymers
based on imine linkage. Both 2D polymers are revealed to be 2D organic semiconductors with band gaps
10 around 1 eV. STM characterization reveals that the rigidity and affinity of building blocks to the surface
has essential effect on the topology of the 2D polymers.

Recently, the synthesis and characterization of two-dimensional polymers has attracted significant interest due to their potential application as nanoporous membranes and electronic, photoelectronic 15 materials.[1-6] In these sheet-like materials the molecular building blocks are linked by covalent bonds into two-dimensional porous crystalline networks, provides robust materials that allow precise control over composition, topology and porosity.[7-9] Unlike graphene, the first prototype of 2D polymers, such 2D polymers constructed by 20 pure organic building blocks have the promise of tuning the properties through rational design and synthesis.[10] The band alignment of such materials can be precisely and predictably controlled by programmable design of the starting materials.[11] The potential to recognize specific target molecules through the 25 incorporation of tailored recognition sites in a highly organized manner to such molecular scale membranes renders 2D polymer extremely attractive in nanosensing.[3]

Different strategies have been developed to prepare 2D polymers with single layer thickness, all rely on the 2D organization of 30 monomers during polymerization.[1-9,12-14] The exfoliation of layer materials offers the possibility to prepare 2D polymers in bulk quantities,[13-14] however, the reachable lateral dimensions of a single sheet, which is crucial for applications in devices, is limited to micrometers. In contrast, the strategy of surface or interface confined 35 reactions offer the possibility to prepare single sheets with macroscale area, which is extremely attractive considering application as nanoporous membranes or in photo-electronics.[4,15-17]

Up to now the tool box toward on-surface synthesis of 2D polymers is quickly expanding owning to the exploration of new reactions.[18] 40 Among all these reactions the Schiff base reaction represents one of the most attractive one because it is the only reaction can give π-conjugated connections apart from Ullmann coupling.[15,19] A outstanding advance for the construction of well-ordered imine 2D polymers were reported by Wan *et al.*[15b] By applying a water 45 background in a autoclave, highly ordered 2D polymers were obtained, which is attributed to the enhanced reversibility of the reaction. However, our own work with an apparently not so

"reversible" reaction condition has resulted in 2D polymers with equal good periodicity,[15a] which highlights that besides the reaction 50 reversibility there are other important factors controlling the quality of 2D polymers obtained via on-surface condensation. Thus, for the rational design and synthesis of high quality 2D polymers, more extensive work to understand the mechanism of on-surface reaction, as well as the chemical, mechanical and electronic properties of 2D 55 polymers are badly in need.[20] In this work, we have investigated the on-surface reaction between 5, 10, 15, 20-meso-tetra(4-aminophenyl) porphine (TAPP) and two dialdehydes with phenyl and quaterthiophene backbones (Scheme 1). Both backbones are in principle rigid, however, the quaterthiophene moiety has more 60 rotational freedoms that can result in diverse conformations.[21] Although extended 2D polymers have been successfully constructed at the water-Au(111) interface by regulating the solution pH using similar building blocks,[15c,19] our results give new insight on the effect of the rigidity and preferential adsorption of monomers on the 65 morphology of on-surface synthesized 2D polymers.
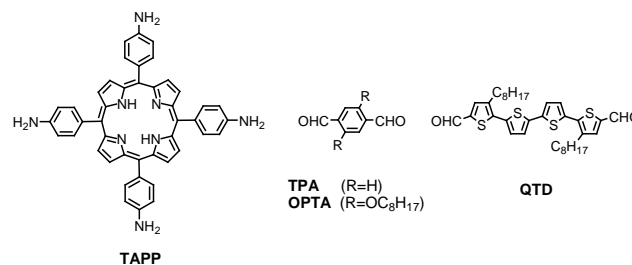
Scheme 1. Chemical structures of the amine and aldehyde precursors: 5, 10, 15, 20-meso-tetra(4-aminophenyl)porphine (TAPP), terephthalaldehyde (TPA) and 2,5-dioctyloxy-terephthalaldehyde (OTPA), 3, 3'''-dioctyl-2, 2': 5', 5": 2", 2'''-quaterthiophene- 5, 5'''- 70 dialdehyde (QTD).

Before the on-surface synthesis, state-of-the-art DFT simulations were carried out first to investigate the feasibility of the structural design and the band structure of the projected 2D polymers. To reduce the demand of resources and accelerate the simulation, the

alkyl/alkoxy chains in both 2D polymers were omitted. The optimized structures are shown in Figure 1a and 1b. The two unit cells are squares with a = b = 25.47 Å for the $2DP_{TAPP–TPA}$ and a = b = 36.55 Å for the $2DP_{TAPP–QTD}$, respectively. $2DP_{TAPP–QTD}$ is more
5 planar than $2DP_{TAPP–TPA}$ due to less repulsion between the thiophene rings. The torsion angles between the porphyrin and phenyl substituents measure 50 ± 1.3° and 49 ± 1.5° for $2DP_{TAPP–TPA}$ and $2DP_{TAPP–QTD}$, respectively, while the phenyl and quaterthiophene backbone of dialdehydes are parallel to the surface.

10 As indicated by the density of states (DOS) (Figure 1c), both $2DP_{TAPP–TPA}$ and $2DP_{TAPP–QTD}$ are semi–conductors with band gap of 1.15 and 1.04 eV, respectively. It is obvious that the conjugation in $2DP_{TAPP–QTD}$ is higher and the extensive conjugation is in favor of narrowing the band gaps. The valence band maximum (VBM) for
15 $2DP_{TAPP–TPA}$ originates mainly from the 2p orbitals of C and N in TAPP and TPA, and the contribution from TAPP is larger than that from TPA, while the conduction band minimum (CBM) essentially originates from both TAPP and TPA (Figure 1d). As for $2DP_{TAPP–QTD}$, the CBM is predominantly contributed by the 2p orbital of C and S in
20 the QTD moiety; in contrast VBM is mainly concentrated on the TAPP moiety, resulting in spatial separation of VBM and CBM (Figure 1e). This is a typical hetero-junction alignment, suggesting an effective spatial carrier separate distribution of electrons and holes, which is important to photovoltaic and other relevant applications.[22]
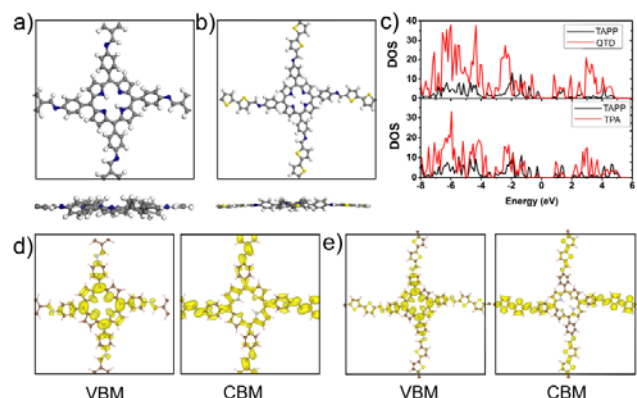

25 **Figure 1.** Top and side view of the DFT optimized geometrical structures of $2DP_{TAPP-TPA}$ (a) and $2DP_{TAPP-QTD}$ (b) in unit cell. (c) The DOS of $2DP_{TAPP-TPA}$ and $2DP_{TAPP-QTD}$ (the Fermi Energy is set to the top of VBM). And the decomposed charge densities of VBM and CBM of $2DP_{TAPP-TPA}$ (d) and $2DP_{TAPP-QTD}$ (e), respectively.

30 The on-surface synthesis of $2DP_{TAPP-OTPA}$ was carried out by applying a mixed solution of the monomers on a freshly cleaved highly oriented pyrolytic graphite (HOPG) substrate and annealing it at 200°C for 30 mins in a vacuum oven, STM characterization reveals extended 2D networks with square lattice (Figure 2). The extended
35 porous 2D polymers nearly cover the full surface. The lateral dimension of the square lattice can extend from 10 to 30 nanometers. Domains of different orientations could be found easily and apparently their orientations are not following the main symmetry axis of graphite, which indicates the weak interaction between
40 $2DP_{TAPP-OTPA}$ and graphite. Curved one dimensional polymer chains due to incomplete reaction can be occasionally observed at domain boundaries (pointed by the white arrow in Figure 2a), which highlight the flexibility of the imine linkage.

In the high resolution image (Figure 2b), the four-lobe brighter
45 protrusions are attributed to the TAPP moieties, while the dimmer

features connecting two protrusions deemed to be the phenyl group of the OTPA and two imine linkages. The distance between TAPP centers measures 2.6 ± 0.1 nm, in good consistence with the DFT simulation of TAPP covalently linked by TPA. Apart from squares,
50 rhombus (Figure 2b, black arrow) can also be observed and this phenomenon is attributed to the flexibility of the imine linkage, the symmetry of the graphite substrate may also play a role in this square to rhombus distortion.[23] The fine resolution of the STM image also enables the detection of defects as highlighted with the blue arrow in
55 Figure 2b, which is attributed to the missing of one OTPA molecule. Similar defects can also be identified at the lower left of the same image. A statistic on the coordination number of TAPP in the 2D polymer shows that the abundance of TAPP with coordination number of four, three, two and one is 32%, 42%, 22% and 4%,
60 respectively. Overall, the extent of reaction has reached a relatively good yield of 75% in terms of amine groups available on the surface.
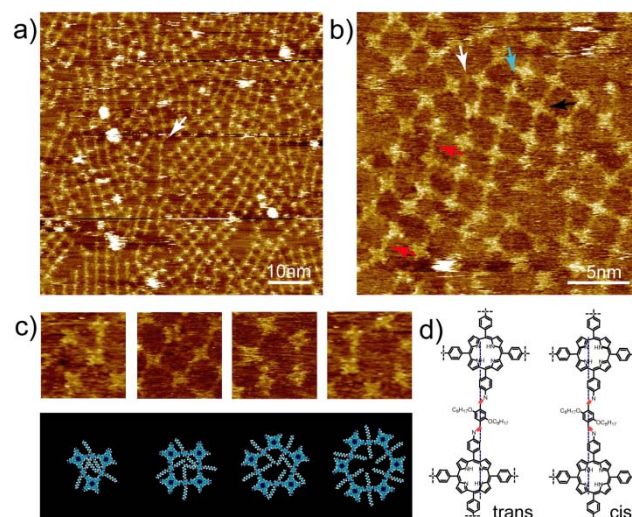

Figure 2. Large scale (a) and high resolution (b) STM images of $2DP_{TAPP-OTPA}$ obtained with the mole ratio of amino : aldehyde = 3 : 1 and 1 : 1, at air-HOPG interface, and the concentrations of TAPP are $1.1 × 10^{-5}$ and
65 $6.8 × 10^{-6}$ mol/L, respectively. The white and black arrow in (b) indicate a triangle and deformed square, respectively, while the blue arrow points to a site where a TPA is missing. The red arrows point to two OTPA linkages with *cis*-conformation. (c) Representative STM images and corresponding models from triangle to hexagon. Tunneling conditions:
70 V_{bias} = 300 mV, I_{set} = 33 pA for (a), V_{bias} = -200 mV, I_{set} = 17 pA for (b). (d) An illustration of the *trans*- and *cis*-conformation of imine linkage.

Even though $2DP_{TAPP-OTPA}$ is composed mostly by squares, at domain boundaries different polygons exist, with triangle as the most frequently detected (Figure 2b). With careful inspection of more high
75 resolution STM images, we found that larger polygons, pentagon and hexagon do also exist and the sites they appear are also near the domain boundaries. Representative STM images and corresponding molecular models of these polygons are shown in Figure 2c. A statistic of the abundance of the polygons clearly indicates tetragons
80 (including squares and rhombus) are the prevailing species, accounting for 78%, followed by triangle, pentagon and hexagon, occupies 17%, 5% and less than 1%, respectively.

In fact the submolecular resolved high resolution image even enables identification of the *cis* and *trans*-conformation of the imine
85 linkage (Figure 2d and Figure S2). Though from an energetic aspect of view $2DP_{TAPP-OTPA}$ with all imine linkages adapting all *trans*-conformation will be most favorable, *cis*-conformation could present in the 2D polymer due to kinetic factors, which has been assumed to

cause irregular 2D network by Schmitz *et al.*[24] However, no direct proof for the existence of different conformations has been presented before. Here we present direct proof of existence of *cis*-conformation of the imine linkage, as indicated by the red arrows in Figure 2b. The four-lobe character of the TAPP moiety allows for precise determination of the orientation of the phenyl groups, thus determining the conformation of the imine linkage (Figure 2b and 2d).

As discussed above the electron density of the CBM of 2DP$_{TAPP-OTPA}$ distributes almost evenly on the skeleton, and in contrast, for VBM, the electron density dominantly distributes on the TAPP moiety. This can also be reflected on the STM image contrast. In the STM images obtained with positive bias (Figure 2a), the whole skeleton of 2DP$_{TAPP-OTPA}$ appears with almost same contrast, while in images obtained with negative bias (Figure 2b), the TAPP moiety appears with much higher contrast, reflecting the electron density distribution of VBM. In some cases, only the TAPP parts were visible, while OTPA could not be revealed at all (Figure S3). Though the direct correlation of STM contrasts with frontier orbitals of conjugated organic molecules and graphene nanoribbons have been reported,[25] this is the first observation of frontier bands of a 2D polymer.
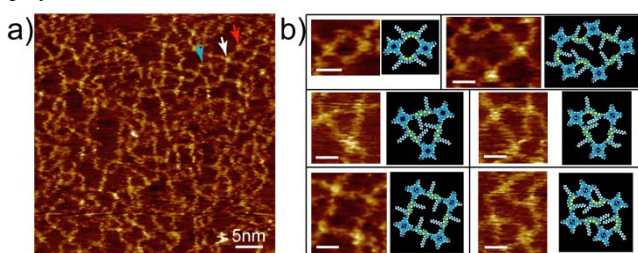

Figure 3. STM images of 2DP$_{TAPP-QTD}$ obtained with the mole ratio of amino : aldehyde = 4 : 1, concentration of TAPP: 1.0×10^{-5} mol/L. Due to the flexibility of QTD the topology of 2DP$_{TAPP-QTD}$ is significantly deformed. (b) High resolution images of the representative polygons and corresponding molecular model. The scale bars in all the images correspond to 2 nm. Tunneling conditions: V$_{bias}$ = -100 mV, I$_{set}$ = 33 pA.

When the alkoxylated monomer OTPA was replaced with terephthalaldehyde (TPA), the porous networks of 2DP$_{TAPP-TPA}$ becomes unstable, easily destroyed by tip scanning (Figure S4), which indicates that the affinity of precursors to substrate does have an effect on the formation and stability of the 2D polymers. The alkoxy chains of OTPA play an important role in stabilizing 2DP$_{TAPP-OTPA}$.

Very different from regular 2DP$_{TAPP-OTPA}$, QTD and TAPP polymerize into irregular networks after annealing at 200℃ for 30 mins (Figure 3a). Due to the flexibility of QTD backbone, the topology of 2DP$_{TAPP-QTD}$ is significantly deformed from the expected square lattice. The four thiophene rings of QTD can rotate freely, resulting in diverse conformations, vary from *all-trans* to *all-cis* (Figure S5). Therefore, regular square network as pointed out by the white arrow in Figure 3a is very rare. Triangle, deformed tetragon, deformed pentagon and even deformed hexagon and heptagons are frequently observed. Another obvious phenomenon in Figure 3 is that not all TAPP vertices are saturated, and parts of the four active amino groups remain intact. A statistic on the coordination number of TAPP vertices demonstrates that the percentage of completely reacted TAPP is 30%, and TAPPs with coordination number of three, two and one are 39%, 25% and 6%, respectively. According to this statistic, in total, 73.3% of the amino groups on the surface have been converted to imines, and this value is very close to that in 2DP$_{TAPP-}$

OTPA. Also the distribution of TAPP with different coordination numbers is very similar in both 2D polymers, further confirms that the difference in topology is originated from the difference in rigidity of dialdehyde monomers.

The high resolution images (Figure 3b) show the details of the representative polygons in 2DP$_{TAPP-QTD}$ with proposed tentative models. The smallest close loop consists two TAPPs as junctions, plus two all-*cis*-conformation QTDs as cambered sides. The regular triangle or square network is composed of QTD edges with *all-trans*-conformation, while in the distorted polygons, the QTD edges are supposed to adopt *cis*-containing conformation. Molecular mechanics simulation indicates in most cases *trans-cis-cis* QTD edges give the most relevant fit. Besides the listed polygons in Figure 3b, some other deformed polygons with six or more edges are also observed (Figure S6), where the flexible QTD backbones adapt various conformations.
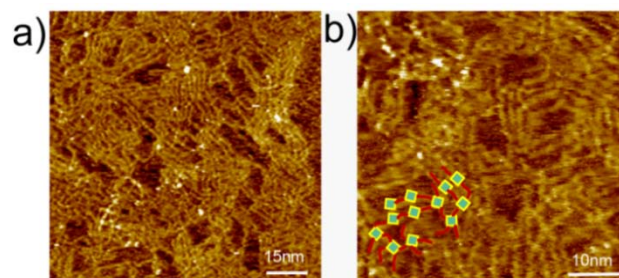

Figure 4. STM images of covalently bonded linear pattern constructed by TAPP and QTD with the mole ratio of amino : aldehyde = 1.5 : 1, concentration of TAPP: 6.6×10^{-6} mol/L. Preferentially adsorption of QTD dominates the resultant liner morphology. Tunneling conditions: V$_{bias}$ = -550 mV, I$_{set}$ = 20 pA.

To have a further insight into the on-surface reaction process, we had varied the mole ratio of precursors (Figure S7). Continuous, relatively ordered 2DP$_{TAPP-OTPA}$ can be formed when the mole ratio of amino to aldehyde group varies from 3:1 to 1:2. Only when TAPP was overdosed too much, the network would become discontinuous. Thus, the on-surface synthesis of 2DP$_{TAPP-OTPA}$ is not very sensitive to the changes of monomer mole ratio. However, as for 2DP$_{TAPP-QTD}$, when the mole ratio of amino and aldehyde group decreased to 1.5 : 1, networks composed of mainly compact linear polymers were observed (Figure 4). Both small regular domains featuring parallel linear polymers and irregular domains characterized by bent and branched lines exist. The majority of TAPPs in this network only reacted with aldehyde through two amino groups on the opposite sides, although TAPPs with coordination number of three or four can also be found as highlighted by the overlaid cartoon in Figure 4b. Similar linear imine polymer of TAPP has been reported previously at the aqueous-gold interface when the concentration of TAPP is high enough.[19] However, in our work, the case seems just opposite. In our case the network-to-linear transition happens when decreasing the concentration of TAPP (from 1.0×10^{-5} mol/L (amino : aldehyde = 4 : 1) to 6.6×10^{-6} mol/L (amino : aldehyde = 1.5 : 1)). According to our previous work, QTD stably adsorbs on the surface,[26] while no stable adlayer of TAPP was observed on the surface of inert HOPG in our experiments, either at room temperature or after annealing. Thus we believe that it is the preferential adsorption of QTD against TAPP leads to the more compact linear packing when increasing the QTD concentration. In case of OTPA, the preference against TAPP is not high enough to lead to compact linear polymers, which is verified by

the fact that stable assembly of OTPA can only be observed with high concentration (Figure S8).

In summary, we have prepared two porphyrin containing 2D polymers, 2DP$_{TAPP-OTPA}$ and 2DP$_{TAPP-QTD}$ through surface confined Schiff based condensation, and studied their chemical and electronic structures via DFT simulation, which confirms that both 2D polymers are organic semiconductors. STM characterization reveals that the topology of the 2D polymers is influenced greatly by the rigidity of precursors. For 2DP$_{TAPP-OTPA}$ we have revealed bias-dependent contrast and correlated it to the spatial distribution of electron density of frontier bands. Our investigation also indicates that the affinity of monomer to HOPG surface has a significant impact on the topology and stability of the 2D polymers. In view of the rich optical and catalytic activity of porphyrin units as well as the possibility of imine to serve as coordination sites, the successful synthesis of porphyrin containing 2D polymers will expand the library of this type of fascinating 2D materials, and open possibilities toward its application in chemical sensing and nanoelectronics.

Notes and references

[a]   X. Sun[§], L. Fan[§], Prof. Dr. S. Lei
State Key Laboratory of Robotics and System, Harbin Institute of Technology, Harbin, 150080, China;
E-mail: leisb@hit.ed.cn
[§]These authors contributed equally to this work

[b]   Dr. X. Zhou, Prof. Dr. W. Q. Tian
State Key Laboratory of Urban Water Resource and Environment, Institute of Theoretical and Simulational Chemistry, Academy of Fundamental and Interdisciplinary Science, Harbin Institute of Technology, Harbin, 150080, China;
E-mail: zhoux@hit.edu.cn

[c]   Dr. Z. Guo, Prof. Dr. Z. Li
School of Polymer Science and Engineering, Qingdao University of Science and Technology, Qingdao 266042, China
E-mail: zxguo@qust.edu.cn

[d]   Dr. X. Li
Key Laboratory of Organo-pharmaceutical Chemistry, Gannan Normal University, Ganzhou, Jiangxi 34100, P. R. China

† Electronic Supplementary Information (ESI) available: [details of any supplementary information available should be included here]. See DOI: 10.1039/b000000x/

[1]   A Gourdon, *Angew. Chem. Int. Ed.* 2008, **47**, 6950-6953.

[2]   D. F. Perepichka, F. Rosei, *Science* 2009, **323**, 216-217.

[3]   N. R. Champness, *Nat. Chem.* **2014**, 6, 757-759.

[4]   S. Clair, O. Ourdjini, M. Abel, L. Porte, *Adv. Mater.* 2012, **24**, 1252-1254.

[5]   (a) R. Bhola, P. Payamyar, D. J. Murray, B. Kumar, A. J. Teator, M. U. Schmidt, S. M. Hammer, A. Saha, J. Sakamoto, A. D. Schlüter, *J. Am. Chem. Soc.* 2013, **135**, 14134-14141; (b) M. Bieri, M. T. Nguyen, O. Gröning, J. Cai, M. Treier, K. Aït-Mansour, P. Ruffieux, C. A. Pignedoli, D. Passerone, M. Kastler, K. Müllen, R. Fasel, *J. Am. Chem. Soc.* 2010, **132**, 16669-16676.

[6]   S. Blankenburg, M. Bieri, R. Fasel, K. Müllen, C. A. Pignedoli, D. Passerone, *Small* 2010, **6**, 2266-2271.

[7]   L. Bartels, *Nat. Chem.* 2010, **2**, 287-295.

[8]   (a) L. Grill, M. Dyer, L. Lafferentz, M. Persson, M. V. Peters, S. Hecht, *Nat. Nanotech.* 2007, **2**, 687-691; (b) M. I. Veld, P. Iavicoli, S. Haq, D. B. Amabilino, R. Raval, *Chem. Commun.* 2008, 1536-1538; (c) N. A. A. Zwaneveld, R. Pawlak, M. Abel, D. Catalin, D. Gigmes, D. Bertin, L. Porte, *J. Am. Chem. Soc.* 2008, **130**, 6678-6679.

[9]   M. Lackinger, W. M. Heckl, *J. Phys. D: Appl. Phys.* 2011, **44**, 464011-464025.

[10]   (a) X. Feng, X. Ding, D. Jiang, *Chem. Soc. Rev.* 2012, **41**, 6010-6022; (b) S. Y. Ding, W. Huang, *Chem. Soc. Rev.* 2013, **42**, 548-568; (c) J. Björk, F. Hanke, *Chem. Eur. J.* 2014, **20**, 928-934; d) J. W. Colson, W. R. Dichtel, *Nat. Chem.* 2013, **5**, 453-465.

[11]   (a) R. Gutzler, D. F. Perepichka, *J. Am. Chem. Soc.* 2013, **135**, 16585-16594; (b) P. Zhu, V. Meunier, *J. Chem. Phys.* 2012, **137**, 244703; (c) Y. Zhou, Z. Wang, P. Yang, X. Zu, F. Gao, *J. Mater. Chem.* 2012, **22**, 16964–16970.

[12]   J. Sakamoto, J. van Heijst, O. Lukin, A. D. Schlüter, *Angew. Chem. Int. Ed.* 2009, **48**, 1030-1069.

[13]   (a) P. Kissel, D. J. Murray, W. J. Wulftange, V. J. Catalano, B. T. King, *Nat. Chem.* 2014, **6**, 774-778; (b) M. J. Kory, M. Wörle, T. Weber, P. Payamyar, S. W. van de Poll, J. Dshemuchadse, N. Trapp, A. D. Schlüter, *Nat. Chem.* 2014, **6**, 779-784.

[14]   (a) I. Berlanga, R. Mas-Ballesté, F. Zamora, *Chem. Commun.* 2012, **48**, 7976-7978; (b) Y. Zhang, M. Tan, H. Li, Y. Zheng, S. Gao, H. Zhang, J. Y. Ying, *Chem. Comm.* 2011, **47**, 7365-7367.

[15]   (a) L. R. Xu, X. Zhou, Y. X. Yu, W. Q. Tian, J. Ma, S. Lei, *ACS Nano* 2013, **7**, 8066–8073; (b) X. H. Liu, C. Z. Guan, S. Y. Ding, W. Wang, H. J. Yan, D. Wang, L. J. Wan, *J. Am. Chem. Soc.* 2013, **135**, 10470-10475; (c) R. Tanoue, R. Higuchi, N. Enoki, Y. Miyasato, S. Uemura, N. Kimizuka, A. Z. Stieg, J. K. Gimzewski, M. Kunitake, *ACS nano* 2011, **5**, 3923-3929.

[16]   K. Seufert, M.-L. Bocquet, W. Auwärter, A. Weber-Bargioni, J. Reichert, N. Lorente, J. V. Barth, *Nat. Chem.* 2011, **3**, 114-119.

[17]   (a) J. F. Dienstmaier, D. D. Medina, M. Dogru, P. Knochel, T. Bein, W. M. Heckl, M. Lackinger, *ACS Nano* 2012, **6**, 7234-7242; (b) C. Z. Guan, D. Wang, L. J. Wan, *Chem. Commun.* 2012, **48**, 2943-2945.

[18]   (a) S. Weigelt, C. Busse, C. Bombis, M. M. Knudsen, K. V. Gothelf, E. Læsgaard, F. Besenbacher, T. R. Linderoth, *Angew. Chem. Int. Ed.* 2008, **47**, 4406 –4410; (b) H. Zhou, J. Liu, S. Du, L. Zhang, G. Li, Y. Zhang, B. Z. Tang, H. J. Gao, *J. Am. Chem. Soc.* 2014, **136**, 5567-5570; (c) H. Y. Gao, P. A. Held, M. Knor, C. Mück-Lichtenfeld, J. Neugebauer, A. Studer, H. Fuchs, *J. Am. Chem. Soc.* 2014, **136**, 9658-9663; (d) A. C. Marele, R. Mas-Ballestè, L. Terracciano, J. Rodríguez-Fernández, I. Berlanga, S. S. Alexandre, R. Otero, J. M. Gallego, F. Zamora, J. M. Gómez-Rodríguez, *Chem. Comm.* 2012, **48**, 6779-6781.

[19]   (a) R. Tanoue, R. Higuchi, K. Ikebe, S. Uemura, N. Kimizuka, A. Z. Stieg, J. K. Gimzewski, M. Kunitake, *J. Nanosci. Nanotechnol.* 2014, **14**, 2211-2217; (b) M. Kunitake. R. Higuchi, R. Tanoue, S. Uemura, *Curr. Opin. Colloid Interface Sci.* 2014, **19**, 140–154.

[20]   (a) J. Adisoejoso, T. Lin, X. S. Shang, K. J. Shi, A. Gupta, P. N. Liu, N. Lin, *Chem. Eur. J.* 2014, **20**, 4111-4116; (b) E. A. Lewis, C. J. Murphy, M. L. Liriano, E. C. H. Sykes, *Chem. Comm.* 2014, **50**, 1006-1008; (c) A. Ciesielski, M. El Garah, S. Haar, P. Kovaříček, J. M. Lehn, P. Samorì, *Nat. Chem.* 2014, **6**, 1017-1023.

[21]   X. Sun, J. Zhang, X. Wang, C. Zhang, P. Hu, Y. Mu, X. Wan, Z. Guo, S. Lei, *Chem. Commun.* 2013, **49**, 10317-10319.

[22]   (a) T. M. Clarke, J. R. Durrant, *Chem. Rev.* 2010, **110**, 6736-6767;(b) S. Guenes, H. Neugebauer, N. S. Sariciftci, *Chem. Rev.* 2007, **107**, 1324-1338; (c) X. Guo, M. Baumgarten, K. Müllen, *Prog. Polym. Sci.* 2013, **28**, 1832-1908.

[23]   Z. Shi, N. Lin, *J. Am. Chem. Soc.* 2010, **132**, 10756–10761.

[24]   C. H. Schmitz, J. Ikonomov, M. Sokolowski, *J. Phys. Chem. C* 2011, **115**, 7270–7278.

[25]   (a) P. Järvinen, S. K. Hämäläinen, K. Banerjee, P. Häkkinen, M. Ijäs, A. Harju, P. Liljeroth, *Nano Lett.* 2013, **13**, 3199-3204; (b) H. H. Yang, Y. H. Chu, C. Lu, T. H. Yang, K. J. Yang, C. C. Kaun, G. Hoffmann, M. T. Lin, *ACS nano* 2013, **7**, 2814-2819.

[26]   QTD can assembly into long range well-ordered lamella structure on the surface of HOPG as reported previously (X. L. Sun, Y. Mu, J. Zhang, X. Wang, P. Hu, X. Wan, Z. Guo, S. Lei, *Chem.-Asian J.* 2014, **9**, 1888-1894). OTPA can also form stable assembly due to the stabilization effect of alkoxy chains (see supporting information). However, TPA and TAPP cannot form stable assembly at either solid-liquid or solid-air interface.